

Supercritical CO₂ Assisted Drug Loading and Degradation Behavior and Osteogenicity of Magnesium Alloy Matrix Calcium-Phosphorus-Chitosan-Graphene Oxide Bone Material

Jie Zhang^{1*}, Shaochun Lv², Shujing Zhou¹, Hongbin Qiu^{3**}, Huiming Zhang², Jinjing Li¹, Ying Wang¹, Xiangyu Zhang¹

¹ Pharmacy Institute, Jiamusi university, Jiamusi 154007, China

² Basic Medical College, Jiamusi university, Jiamusi 154007, China

³ Public Health Institute, Jiamusi university, Jiamusi 154007, China

*E-mail: zjie612@163.com, qiu hongbin@jmsu.edu.cn

Received: 9 September 2019 / Accepted: 28 October 2019 / Published: 31 December 2019

The aspirin(ASA) was loaded on the graphene oxide(GO) by SC-CO₂(supercritical CO₂) method and GO/ASA complex was obtained, then the CaP-CS-GO/ASA(calcium-phosphorus-chitosan-graphene oxide/aspirin) coating was deposited on the magnesium alloy matrix by electrophoresis. The degradation behavior of magnesium alloy matrix CaP-CS-GO/ASA by SC-CO₂ drug loading was studied by immersion experiment. The effects of the soaking solution and material coating on the proliferation of mouse osteoblasts 3T3E1 in vitro were detected by CCK-8 method. The results showed that the corrosion reaction of the magnesium alloy matrix CaP-CS-GO/ASA by SC-CO₂ drug loading in m-SBF was orderly controlled by electrochemical and finite-layer diffusion processes, charge transfer and semi-infinite diffusion processes with the increase of the immersion time. The ASA presence in the CaP-CS-GO coating promoted the proliferation, adhesion and growth of osteoblasts, and the obtained bone material had the good osteogenesis.

Keywords: Magnesium alloy matrix, degradation behavior, graphene oxide, coating, proliferation of osteoblasts

1. INTRODUCTION

As a common metal bone implant, magnesium and magnesium alloys were degradable in biological environment, and unabsorbed magnesium can be excreted in the urine. However, at present, magnesium alloy implants were not widely used in clinical practice, mainly due to their active chemical properties, so that they could be rapidly metabolized in internal environment, which could produce a lot of hydrogen and cause emphysema of tissue. Therefore, the wide application of magnesium alloy as bone implant material was limited[1,2].

The structure of hydroxyapatite(HA) was very similar to the inorganic components of the bones and the teeth in the human body[3-8]. It was no toxic and side effects after implanting in the body, and bone growth and conduction could be achieved while it was safe. The mechanism was that the newborn bone grew on the surface or inside of the implant at a position where the implanted hydroxyapatite combined with the autologous bone[9]. Chitosan(CS) was similar to the structure of organic components in human bones, and the material was easy to degrade. It has excellent biocompatibility, as well as non-toxic and non-irritating[10-12]. Thus, this study was based on the structure of natural bone, and the calcium phosphorus and chitosan were coated to the surface of magnesium alloy matrix, and magnesium alloy matrix CaP-CS bone implant was prepared on the basis of ensuring that the implant presented as the certain mechanical properties. It could not only solve the problem of fast degradation speed of magnesium alloy matrix, but also made the bioactivity and biocompatibility of implant meeting the human's needs. In order to give better performance to the ceramic coating layer, secondary components were usually added to the coating layer. Graphene oxide(GO) had a large number of active chemical groups, such as carboxyl groups, carbonyl groups, hydroxyl groups, and epoxy groups. The presence of these groups could play a role in the adsorption and sustained release of drugs[13,14]. Aspirin was a type of antipyretic, analgesic and anti-inflammatory drug, and small doses of aspirin could resist thromboembolism. In recent years, aspirin has been found to improve bone density in rats[15,16]. Supercritical CO₂(SC-CO₂), which had the advantages of zero surface tension and the disappearance of the gas-liquid interface, could avoid pollution or separation problems of solvents in conventional methods if SC-CO₂ was used for the drug loading[17,18].

Based on the above, the drug of aspirin was loaded on GO by SC-CO₂ technology, and a new type of magnesium alloy matrix CaP-CS-GO/ASA bone implant by SC-CO₂ carrier was built. This had a certain practical significance on enriching the types of the degradable magnesium alloy implants and developing new functional bone implants.

2. EXPERIMENTAL METHODS

2.1 Graphene oxide loading with aspirin

Physical method: 10mg GO was dispersed in 30ml absolute ethanol for 40 minutes under ultrasound to obtain GO dispersion solution. 10mg aspirin was added into the dispersing solution and mixture was stirred for 2 hours at the temperature of 20°C, then filtrated by the microporous membrane and dried at room temperature.

SC-CO₂ method: GO was taken as carrier for the drug loading by using the supercritical CO₂ extraction device. Firstly, 10mg GO was placed in the extraction tank of the supercritical extraction device(HA-221-50-06, China). 20mg aspirin was dissolved in absolute ethanol, and this solution was transferred to the entrainer tank of the supercritical extraction device, mixing with SC-CO₂ through a pump in the mixer. Aspirin solution was carried into the extraction tank by SC-CO₂ through a purifier. When the aspirin solution contacted with GO in the extractor, SC-CO₂ carried the anhydrous ethanol into the separator. In the separator, absolute ethanol remained in the separator because SC-CO₂ changed to normal CO₂, and CO₂ was recycled until the end of drug loading. The pressure and temperature of the extraction tank were adjusted at

20Mpa and 40°C respectively, loading it for 1 hour, then the drug-loaded products(GO-ASA compound) could be dried at room temperature for 24 hours.

2.2 Pretreatment of magnesium alloy matrix

AZ91D magnesium alloy was cut into magnesium alloy blocks with a size of 1cm×1cm×0.5cm. The block of the magnesium alloy was connected by one end of the wire. The magnesium alloy was encapsulated with epoxy resin and polyamide(the volume ratio was 1:1) so that it could be exposed to only one surface of 1cm². Then the surface of the magnesium alloy was polished by different number of sandpaper, and finally cleaned by ultrasonic. Finally, the magnesium alloy was treated by the micro-arc oxidation for 10 seconds[14,15].

2.3 Preparation of magnesium alloy matrix CaP-CS-GO/ASA bone material

CaP-CS coating, CaP-CS-GO/ASA coating by physical drug loading and CaP-CS-GO/ASA coating by SC-CO₂ drug loading were deposited on magnesium alloy matrix by a electrophoresis, respectively[19]. In the electrophoresis solution of 500ml, the volume ratio of the acetic acid aqueous solution to absolute ethanol solution was 2:3. Specifically, 0.25g chitosan(CS) and 1.0g nHA particles were added to 200ml acetic acid aqueous solution(acetic acid of 9ml) under ultrasonic condition to obtain solution A. Then 1.5g nHA particles and 0.05g GO-ASA compound obtained by physical method (or GO-ASA compound by SC-CO₂ method) were added to 300ml absolute ethanol under ultrasonic condition to obtain suspension B. A and B were mixed, treated by the ultrasound for 1~2 hours and aged for 24 hours. In the electrophoresis process, AZ91D magnesium alloy was the cathode, and Ti alloy coated by iridium and tantalum was the anode. The distance between the two electrodes was about 1cm. The electrophoresis process was performed at constant voltage 40V for 20-40 minutes.

The prepared magnesium alloy matrix CaP-CS, magnesium alloy matrix CaP-CS-GO/ASA by physical drug loading and magnesium alloy matrix CaP-CS-GO/ASA by SC-CO₂ drug loading were soaked respectively in 250ml phosphate buffer solution for 3~5 days at the temperature of 37°C, the phosphate buffer solution should be replaced every day[20,21]. Then the above materials could be taken out, and rinsed by distilled water, dried at room temperature.

2.4 Immersion experiment

The prepared magnesium alloy matrix CaP-CS, magnesium alloy matrix CaP-CS-GO/ASA by physical drug loading and magnesium alloy matrix CaP-CS-GO/ASA by SC-CO₂ drug loading were respectively soaked in 250ml simulated body fluid(m-SBF) at 37°C. The solid samples were took out at different time of soaking, then dried and used for the bioactivity experiments. The m-SBF immersion solutions of three materials were sealed and preserved for the cell experiments.

Meanwhile, magnesium alloy matrix CaP-CS-GO/ASA by SC-CO₂ drug loading sample were soaked in 250ml m-SBF. The pH value of the soaking solution was determined at 1, 3, 6, 8, 10 and 12 weeks respectively, and the electrochemical test of solid sample was carried out as the following methods.

2.5 Degradation Experiment

2.5.1 Electrochemical impedance measurement

The samples of magnesium alloy matrix CaP-CS-GO/ASA by SC-CO₂ drug loading were tested by electrochemical impedance spectroscopy(EIS) through using traditional three-electrode system[22,23]. Saturated calomel electrode(SCE) was used as a reference electrode, platinum plate as a counter electrode, the sample as the working electrode and m-SBF as the test medium. The system was kept the stable for 20 minutes at 37°C before the test. The frequency range was from 100KHz to 10MHz and the amplitude was 5mV. The equivalent circuit was fitted by Zsimp Win(3.0) software for EIS results.

2.5.2 Potentiodynamic polarization measurement

The samples of magnesium alloy matrix CaP-CS-GO/ASA by SC-CO₂ drug loading at different soaking time were measured by potentiodynamic polarization measurement[24]. The scanning rate was 0.005V per-second and the polarization time was 2 seconds.

2.6 Biological activity test

2.6.1 Effect of the soaking solution on the osteoblast proliferation by CCK-8 method

Mouse osteoblasts 3T3E1 at the logarithmic growth phase was cultured in 96-well plates after the trypsinization and the cell concentration was adjusted to $4 \times 10^5 \text{ml}^{-1}$. All of the cells were divided into three groups: the soaking solution group of magnesium alloy matrix CaP-CS, the soaking solution group of magnesium alloy matrix CaP-CS-GO/ASA by physical drug loading and the soaking solution group of magnesium alloy matrix CaP-CS-GO/ASA by SC-CO₂ drug loading. A certain amount of the mixed liquid of experimental material soaking solution and conventional culture solution was added into each pore as a new complete cell culture medium. The content of soaking solution was 10%, 20%, 30%, 40%, 50%, 60%, 70%, 80%, 90% and 100% respectively, and the total liquid volume of each pore was kept at 100ml. The blank control pore should also be set up. The blank pore was laid with the osteoblasts 3T3E1 and the conventional culture medium was added into it. Five duplicated pores were set up under each condition in each group. Three groups of cells were placed in the incubator at 37°C and 5%CO₂. After 24 hours of incubation, 10μL CCK-8 solution was added into each pore. After 3 hours of the full reaction, the absorbance of each pore at 490nm was measured by ELISA, and the proliferation index was calculated by the following formula (1).

$$\text{Proliferation Index(\%)} = \frac{\text{The average OD value of the experimental group} - \text{The average OD value of the control group}}{\text{The average OD value of the control group}} \times 100\% \quad (1)$$

2.6.2 Effect of the soaking time on the osteoblast proliferation by CCK-8 method

The cell groups were divided as follows in 2.6.1. The effects of soaking solution on the proliferation index of osteoblasts were investigated at 1, 2, 4, 6, 8, 10 and 12 weeks respectively.

2.6.3 Effect of the cell culture time on the osteoblast proliferation by CCK-8 method

2.6.3.1 Taking soaking solution as cell culture medium

The cell groups were divided as follows in 2.6.1. The proliferation index of osteoblasts was observed at 8, 10, 12, 20, 24 and 48 hours, respectively.

2.6.3.2 Taking coating as cell growth matrix

CaP-CS coating, CaP-CS-GO/ASA coating by physical drug loading, CaP-CS-GO/ASA coating by SC-CO₂ drug loading were treated and laid at the bottom of 24-well plate in parallel. Then the osteoblasts 3T3E1 of mice in the logarithmic growth phase were picked up and digested by trypsinase. The cell concentration was adjusted by $4 \times 10^5 \text{ml}^{-1}$. The cells were inoculated into the well plate with the conventional culture medium of 1000 μL per well. Meanwhile, the blank orifice was set up, and it was not laid with cells. Three duplicated wells were set up under each condition in each group. These 24-well plates were put into incubator at 37°C and 5% CO₂. After incubation for a certain period of time, the remained liquid was removed from the well plate, then washed with PBS for 1~2 times and digested by trypsin for 1 minute. The conventional medium was added to each well and the cells in each well were blowed. The prepared cell suspension was transferred into 96-well plate and fully reacted with 10 μl CCK-8 solution for 4 hours. The absorbance values of each well at 490nm were determined by ELISA, and the proliferation index was calculated with the same formula(1). The proliferation index of four groups was observed at 12, 24 and 48 hours, respectively. For the CaP-CS-GO/ASA coating groups, the proliferation index was observed when the cell culture time was extended to 1, 2 and 3 days.

2.6.4 Laser confocal experiment

CaP-CS coating, CaP-CS-GO coating, CaP-CS-GO/ASA coating by physical drug loading and CaP-CS-GO/ASA coating by SC-CO₂ drug loading were placed in 24-well plate respectively. The osteoblasts 3T3E1 in logarithmic growth phase were picked up and inoculated with $4 \times 10^5 \text{ml}^{-1}$. After incubation for 24 hours, the well plate was fixed in the incubator for 10 minutes by adding 4% polyformaldehyde of 0.2ml into each well at 37°C and 5% CO₂. After 10 minutes, the fixed solution was sucked out, the well plate was washed with PBS and 0.5% Triton X-1000 of 5ml was added. The rhodamine ghostpen ring peptide of 200 μl was added and kept in darkroom at room temperature for 40 minutes, then the well plate was rinsed by PBS and sealed with fluorescent quenching agent. After treatment, it was placed on the the platform of laser confocal microscope and scanned to observe the growth of osteoblasts.

3. RESULTS AND DISCUSSION

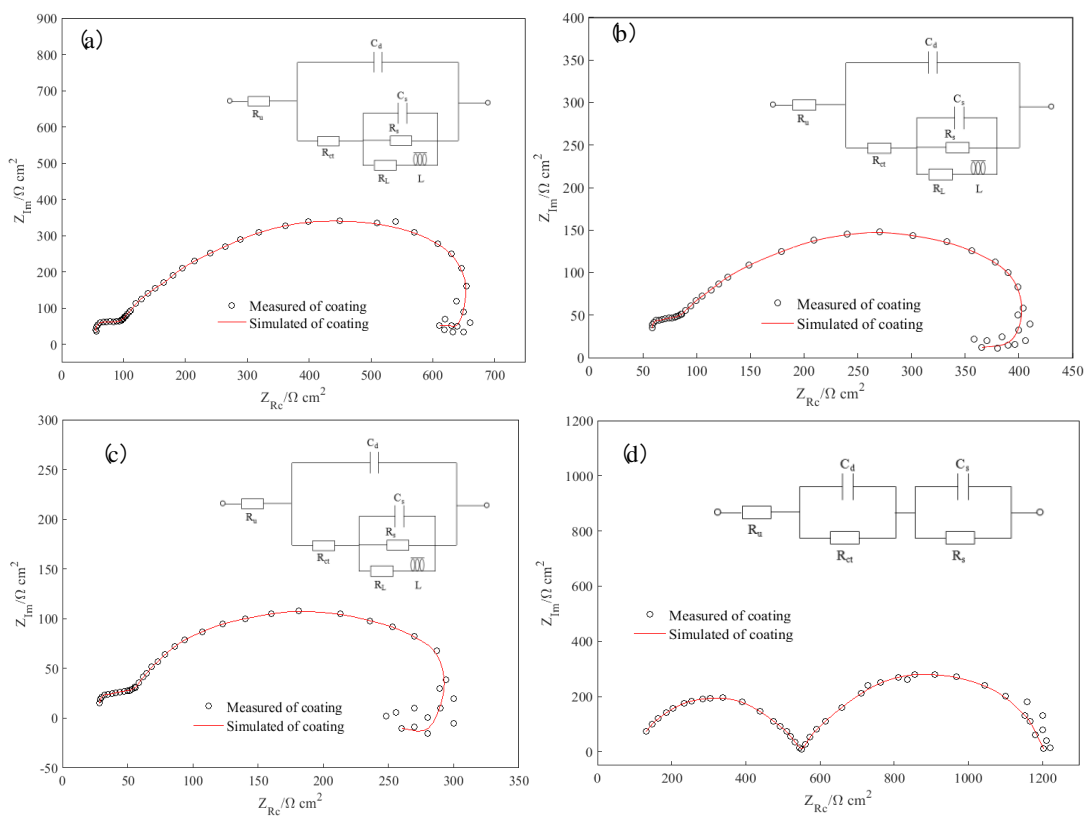
3.1 Degradation behavior

Fig.1 showed the Nyquist plots and equivalent circuits of magnesium alloy matrix CaP-CS-GO/ASA by SC-CO₂ drug loading immersed in m-SBF for different times[21,25]. Nyquist plots of Fig.1(a), Fig.1(b) and Fig.1(c) were similar, they were composed of two capacitive reactance arcs at the high and medium frequencies and one inductive reactance arc at the low frequency. It could be seen from Fig.1(d) that the Nyquist plot was composed of two capacitive reactance arcs. The capacitive reactance arc in the high-frequency region represented the charge transfer resistance(R_{ct}) and interface electrical double-layer capacitance(C_d). While the capacitive reactance arc in the intermediate frequency region represented the resistance(R_s) and membrane capacitance(C_s) when the m-SBF went across the surface of corrosion product layer of magnesium alloy, the MAO layer and the CaP-CS-GO/ASA coating, which was caused by the finite layer diffusion. The low-frequency reactive arc represented the adsorption and separation of the corrosion products at the interface between solution and metal matrix, such as $Mg(OH)_2$ [26-28].

When the magnesium matrix CaP-CS-GO/ASA by SC-CO₂ drug loading was soaked in m-SBF for 1 week (Fig.1(a)), 3 weeks (Fig.1(b)) and 6 weeks (Fig.1(c)), the Nyquist plots were composed of two capacitive reactance arcs at the high-medium frequency region and one inductance arc at the low frequency region. The corrosion reaction of the sample was controlled by the electrochemical and finite layer diffusion processes, accompanying with the adsorption and detachment of the corrosion products on the matrix. When the magnesium alloy matrix CaP-CS-GO/ASA by SC-CO₂ drug loading was soaked in m-SBF for 8 weeks (Fig.1(d)), the Nyquist plots were composed of two capacitive reactance arcs, and the corrosion reaction of the sample was controlled by electrochemical and finite layer diffusion processes. As it was soaked in m-SBF for 10 weeks (Fig.1(e)) and for 12 weeks (Fig.1(f)), the Nyquist plots were composed of a capacitive reactance arc in the high-frequency region and a diagonal line in the middle and low frequencies. The capacitive reactance arc in the high-frequency region represented the process of charge transfer, while the diagonal line in the middle and low frequencies was caused by the semi-infinite diffusion process. When the sample was soaked in m-SBF, m-SBF penetrated into the pores in the ceramic coating, corrosion preferentially occurred in MAO, and only capacitive reactance arc in the high frequency appeared in the impedance spectrum. Due to the biological activity of the CaP-CS-GO/ASA coating, phosphate deposition process and weak dissolution process existed. The CaP-CS-GO/ASA coating layer played a major protective role on the magnesium alloy matrix, meanwhile, MAO layer and its corrosion products layer also had certain protective effect on magnesium alloy matrix. The protective effect of CaP-CS-GO/ASA coating, MAO layer and its corrosion products layer on the metal matrix corresponded to the capacitive reactance arc of the middle frequency region in the impedance spectrum. In addition, the formation and detachment processes of corrosion products on magnesium alloy matrix corresponded to the induction reactance arc of the low frequency region in the impedance spectrum. With the extension of soaking time, some corrosion products were precipitated at the interface of MAO layer and CaP-CS-GO/ASA coating. As a result, the surface of the oxide layer on magnesium matrix appeared some cracks, eventually leading to the severe pitting corrosion and filiform corrosion on the surface of magnesium alloy, making the CaP-CS-GO/ASA coating gradually broken. Thus, the capacitive and inductive reactance arcs disappeared, and the slant line appeared in the middle and low

frequency regions(Fig.1(e)(f)). Specifically, when magnesium alloy matrix CaP-CS-GO/ASA by SC-CO₂ drug loading was soaked in m-SBF from 1 week to 6 weeks(Fig.1(a)(b)(c)), there were some micropores and gaps in the CaP-CS-GO/ASA coating, which enabled the m-SBF to contact with the metal matrix and react with it. The generated corrosion products would be covered on the metal matrix, making the electrochemical reaction difficultly produce, to some extent, it could protect the matrix material and make R_{ct} increase while R_s decrease.

When the soaking time in m-SBF reached 8 weeks (Fig.1(d)), corrosion products generated on magnesium alloy matrix and filled the pores between MAO layer and CaP-CS-GO/ASA coating, and the protective effect of composite coating on metal matrix was enhanced, and the corrosion rate was slightly reduced, so that R_{ct} decreased while R_s increased. When it was soaked in m-SBF from 10 weeks to 12 weeks(Fig.1(e)(f)), the CaP-CS-GO/ASA coating began to appear the tiny fractures, making the contact area between m-SBF and the MAO layer as well as its corrosion product layer increase. Thus, the corrosion process of metal matrix became easy to occur, leading to the gradual destruction of the CaP-CS-GO/ASA coating that played a major protective role, and the reduction of R_s to zero. Meanwhile, the corrosion products and phosphate deposits existed on magnesium matrix, and the sediments had still a protective effect on the metal matrix, so R_{ct} changed little, as shown in Tab.1.



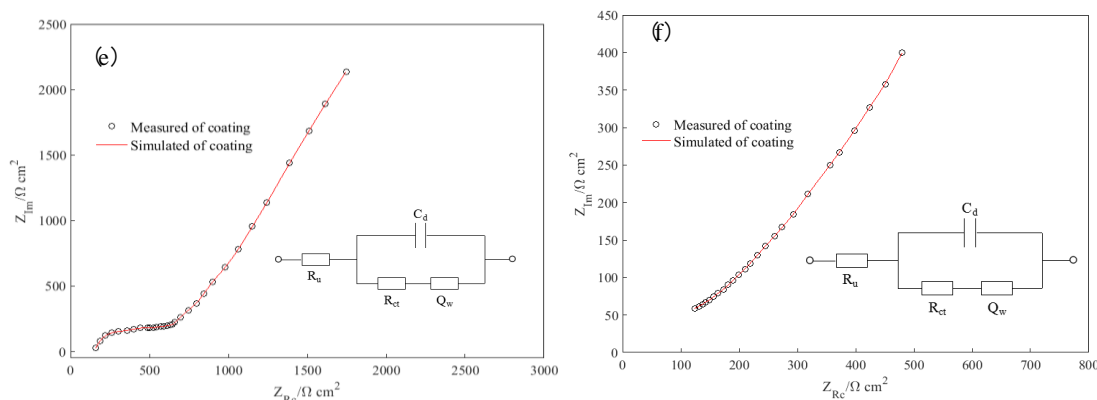


Figure 1. Nyquist diagram and equivalent circuit magnesium alloy matrix CaP-CS-GO/ASA by SC-CO₂ drug loading for different immersion time: (a)1w; (b)3w; (c)6w; (d)8w; (e)10w; (f)12w

Table 1. Fitting results of equivalent circuit for magnesium alloy matrix CaP-CS-GO/ASA by SC-CO₂ drug loading immersed in m-SBF for different time

Time(week)	1	3	6	8	10	12
$R_{ct}/\Omega \cdot \text{cm}^2$	246.97	256.94	728.9	635.2	754	840
$R_s/\Omega \cdot \text{cm}^2$	2403	770	897	1203	0	0

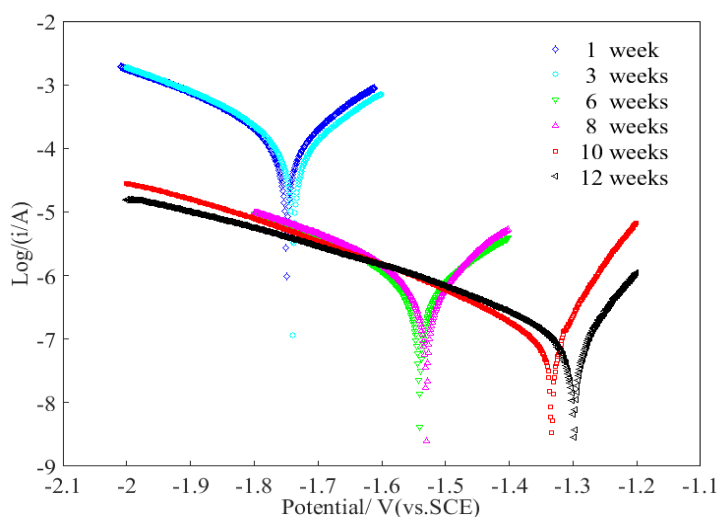


Figure 2. The potentiodynamic polarization measurement for magnesium alloy matrix CaP-CS-GO/ASA by SC-CO₂ drug loading immersed in m-SBF at different time

Fig.2 and Tab.2 showed the potentiodynamic polarization measurement and the analysis results of magnesium alloy matrix CaP-CS-GO/ASA by SC-CO₂ drug loading, which was soaked in m-SBF for different times. As shown in Fig.2 and Tab.2, when the soaking time was extended from 1 week to 12 weeks, the i_{corr} value of corrosion current tended to decrease generally. Specifically, when the soaking time was from 1 week to 6 weeks, the i_{corr} value did not change much and the electrochemical corrosion rate was relatively

stable, because the ceramic coating has not been destroyed. When the soaking time was from 6 to 8 weeks, the i_{corr} value and corrosion rate were slightly reduced, due to the precipitation of corrosion products filled the pores between the MAO layer and the ceramic coating. When the soaking time was from 8 to 12 weeks, the local rupture of the ceramic coating occurred. The metal matrix directly contacted with the m-SBF, which resulted in generating a dense corrosive product coating on the surface of magnesium alloy, so the i_{corr} value and corrosion rate decreased.

Table 2. Potentiodynamic polarization measurement analysis for magnesium alloy matrix CaP-CS-GO/ASA by SC-CO₂ drug loading by SC-CO₂ loading immersed in m-SBF at different time

Time(week)	1	3	6	8	10	12
$E_{corr}/V(vs \cdot SCE)$	-1.760	-1.753	-1.557	-1.539	-1.354	-1.302
$i_{corr}/A \cdot cm^{-2}$	4.3×10^{-5}	4.25×10^{-5}	3.9×10^{-5}	3.2×10^{-5}	5.1×10^{-7}	2.1×10^{-7}
CR / mm yr ⁻¹	0.633	0.730	0.832	0.587	0.032	0.004

Fig.3 illustrated the changes of pH values in the m-SBF for magnesium alloy matrix CaP-CS-GO/ASA by SC-CO₂ drug loading. The results showed that the pH value slightly increased during the whole soaking period, which indicated that the CaP-CS-GO/ASA coating could not prevent the corrosion of magnesium alloy in m-SBF, but only slowed down the corrosion rate of magnesium alloy.

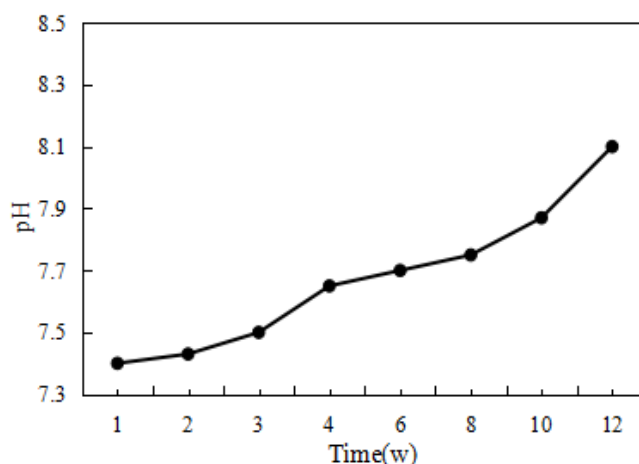


Figure 3. pH values for magnesium alloy matrix CaP-CS-GO/ASA by SC-CO₂ drug loading immersed in m-SBF at different time

3.2 Change of the proliferation index of osteoblasts with different amount of soaking solution

After different amount of soaking solution was applied to the osteoblasts for 24 hours, formula(1) was used to calculate the proliferation index, as shown in Fig.4. Besides, for the magnesium alloy matrix CaP-CS and magnesium alloy matrix CaP-CS-GO/ASA by the physical drug loading(Fig.4(a)(b)), the soaking solution content was 20% when the proliferation index was the lowest. For soaking solution group of magnesium alloy

matrix CaP-CS-GO/ASA by SC-CO₂ drug loading(Fig.4(c)), the soaking solution content was 30% when the proliferation index was the lowest. When the proliferation index in the soaking solution of three groups was the highest, the content of soaking solution was 50%. Meanwhile, the highest proliferation index were respectively 43% and 46% for magnesium alloy matrix CaP-CS and magnesium alloy matrix CaP-CS-GO/ASA by the physical drug loading. The highest proliferation index was 58% for magnesium alloy matrix CaP-CS-GO/ASA by SC-CO₂ drug loading. It could be seen that when the soaking solution content of the three materials was 50%, the proliferation index was the highest. The volume ratio of the soaking solution and cell supernatant in the subsequent cell experiments was 1:1.

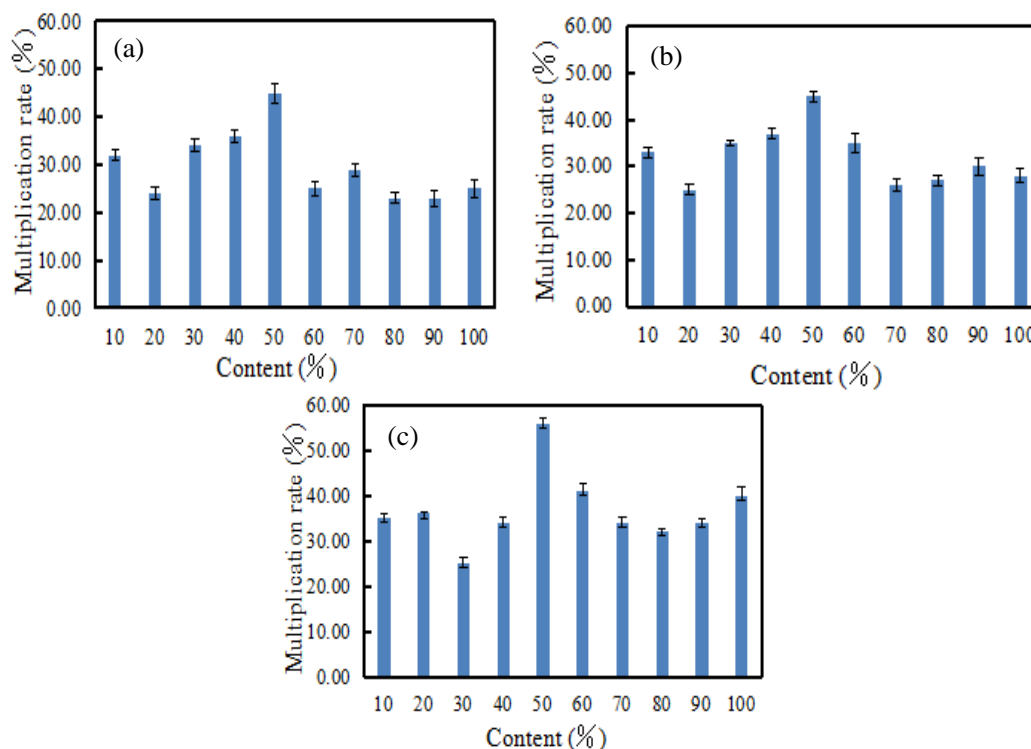


Figure 4. Effects of different soaking solution amount on the proliferation index: (a)magnesium alloy matrix CaP-CS; (b)magnesium alloy matrix CaP-CS-GO/ASA by the physical drug loading; (c)magnesium alloy matrix CaP-CS-GO/ASA by SC-CO₂ drug loading

3.3 Change of the proliferation index of osteoblasts with different soaking time

Formula(1) was used to calculate the effects of the soaking time for different materials on the proliferation index, as shown in Fig.5. According to Fig.5, for three soaking solutions of magnesium alloy matrix CaP-CS, magnesium alloy matrix CaP-CS-GO/ASA by the physical drug loading and magnesium alloy matrix CaP-CS-GO/ASA by SC-CO₂ drug loading, the proliferation index increased and reached the maximum when the soaking time was less than 2 weeks, and the proliferation index gradually decreased when the soaking time increased from 2 weeks to 12 weeks. Meanwhile, when being soaked for 2 weeks, the proliferation index of soaking solution for magnesium alloy matrix CaP-CS was 45%, that of magnesium alloy matrix CaP-CS-GO/ASA by the physical drug loading was 54%, and that of magnesium alloy matrix

CaP-CS-GO/ASA by SC-CO₂ drug loading was 66%. After 12 weeks of soaking, the proliferation index of soaking solution for magnesium alloy matrix CaP-CS was 32%, that of magnesium alloy matrix CaP-CS-GO/ASA by the physical drug loading was 53%, and that of magnesium alloy matrix CaP-CS-GO/ASA by SC-CO₂ drug loading was 60%. Therefore, the soaking time of 2 weeks for the three materials was selected.

In addition, m-SBF was in a static state in the soaking experiment[29,30]. With the extension of soaking time in m-SBF, the release amount of Mg²⁺ continued to increase, which would gradually increase the pH value of the soaking solution, thereby affecting the proliferation ability of cells. Thus, the proliferation index of osteoblasts for three materials' soaking solutions under this condition would be reduced. However, due to the internal environment of human body was different from vitro, so the material was more conducive to cell proliferation and differentiation in vivo[31-33].

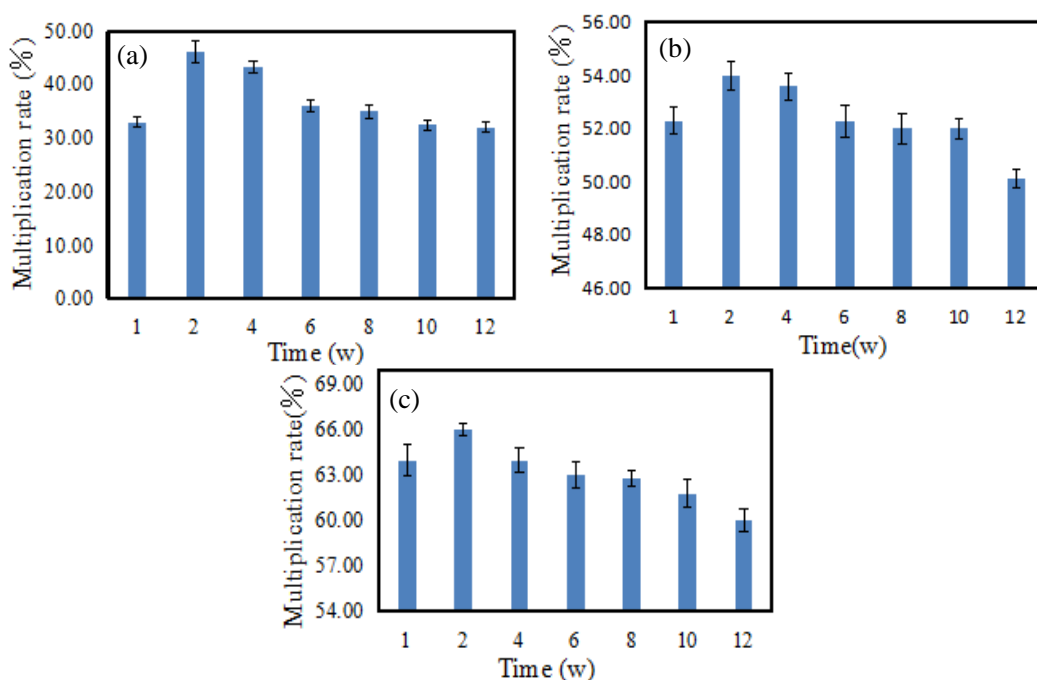


Figure 5. Effects of the soaking time for the immersion liquid of different materials on the proliferation index: (a) magnesium alloy matrix CaP-CS; (b) magnesium alloy matrix CaP-CS-GO/ASA by the physical drug loading; (c) magnesium alloy matrix CaP-CS-GO/ASA by SC-CO₂ drug loading

3.4 Change of proliferation index of osteoblasts with different cell incubating time

3.4.1 Soaking solution as the cell supernatant

The osteoblasts proliferation index was calculated by formula(1), as shown in Fig.6. As shown in Fig.6(a), the proliferation index gradually increased with the extension of incubating time for the soaking solution for magnesium alloy matrix CaP-CS. When the incubating time reached 20 hours, the proliferation index tended to be stable, and the proliferation index was 46% at this time. As shown in Fig.6(b)(c), with the increase of soaking time, the effects of soaking solutions for magnesium alloy matrix CaP-CS-GO/ASA by the physical drug loading and magnesium alloy matrix CaP-CS-GO/ASA by SC-CO₂ drug loading on the

proliferation of osteoblasts showed an increasing trend. In addition, the proliferation index for the two groups of cells were respectively 48% and 59% when the incubating time was 20 hours. The proliferation index reached the highest when the incubating time was 24 hours, the former cell was 55% and the latter cell was 71%. It could be seen that magnesium alloy matrix CaP-CS compound with GO, which had no toxicity to osteoblasts and had good biocompatibility.

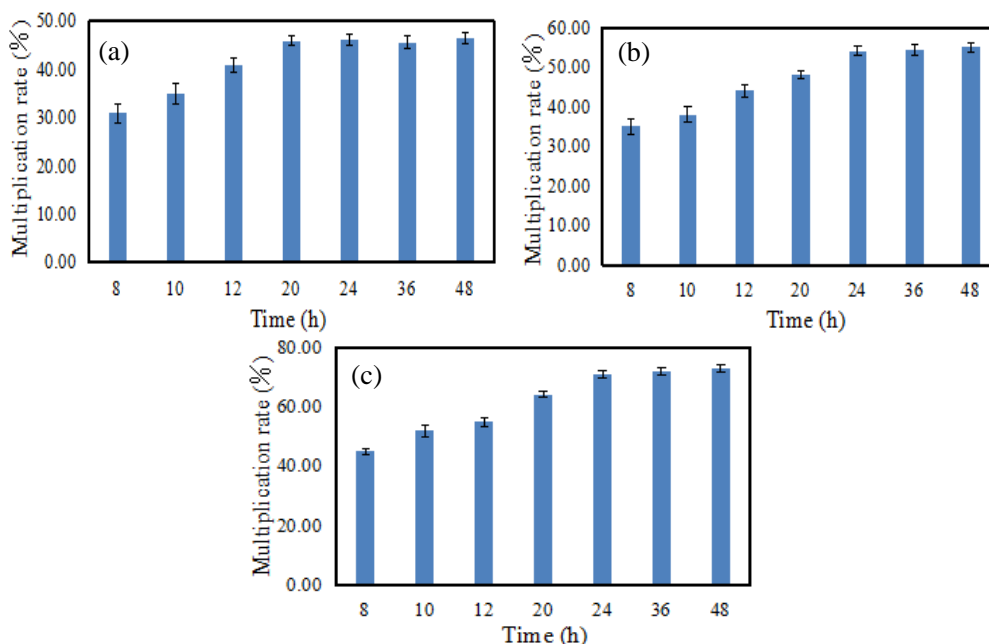


Figure 6. The proliferation index of different incubation time for the immersion liquid of different materials: (a) magnesium alloy matrix CaP-CS; (b) magnesium alloy matrix CaP-CS-GO/ASA by the physical drug loading; (c) magnesium alloy matrix CaP-CS-GO/ASA by SC-CO₂ drug loading

The highest proliferation index of soaking solutions for three materials was in the order of magnesium alloy matrix CaP-CS < magnesium alloy matrix CaP-CS-GO/ASA by the physical drug loading < magnesium alloy matrix CaP-CS-GO/ASA by SC-CO₂ drug loading. Because aspirin was slightly soluble in the aqueous solution, while the drug in magnesium alloy matrix CaP-CS-GO/ASA by the physical drug loading and magnesium alloy matrix CaP-CS-GO/ASA by SC-CO₂ drug loading slowly released when they were soaked in m-SBF. Even more, because aspirin in the soaking solution can promote the proliferation of osteoblasts and inhibit their apoptosis, thus the soaking solution of magnesium alloy matrix CaP-CS-GO loading with drug has better effect of osteoblasts proliferation than that of magnesium alloy matrix CaP-CS-GO[34-36]. Meantime, the loading amount of drug in the prepared GO-ASA compound by SC-CO₂ technology was higher than that of physical method in the previous studies. Therefore, the proliferation effect of osteoblasts in the the soaking solution for magnesium alloy matrix CaP-CS-GO/ASA by SC-CO₂ drug loading was better than that in the magnesium alloy matrix CaP-CS-GO/ASA by the physical drug loading.

3.4.2 Coating as cell growth matrix

The proliferation index was calculated according to formula 1, and the results were shown in Fig.7. It

could be seen from Fig.7(a)(b)(c)(d) that when the culture time increased from 12 hours to 48 hours, the proliferation index of CaP-CS coating, CaP-CS-GO coating, CaP-CS-GO/ASA coating by the physical drug loading and CaP-CS-GO/ASA coating by SC-CO₂ drug loading all showed an increasing trend. When incubation time was 48 hours, the proliferation index was 71% in CaP-CS coating group, 78% in CaP-CS-GO coating group, 142% in CaP-CS-GO/ASA coating by the physical drug group and 185% in CaP-CS-GO/ASA coating by SC-CO₂ drug loading group. Compared with CaP-CS coating, the proliferation index of CaP-CS-GO/ASA coating by the physical drug increased by 50%, and that of CaP-CS-GO/ASA coating by SC-CO₂ drug loading increased by 62%. It could be seen that the loaded ASA in the CaP-CS-GO coating could promote the proliferation, adhesion and growth of osteoblasts, and CaP-CS-GO coating has good biocompatibility.

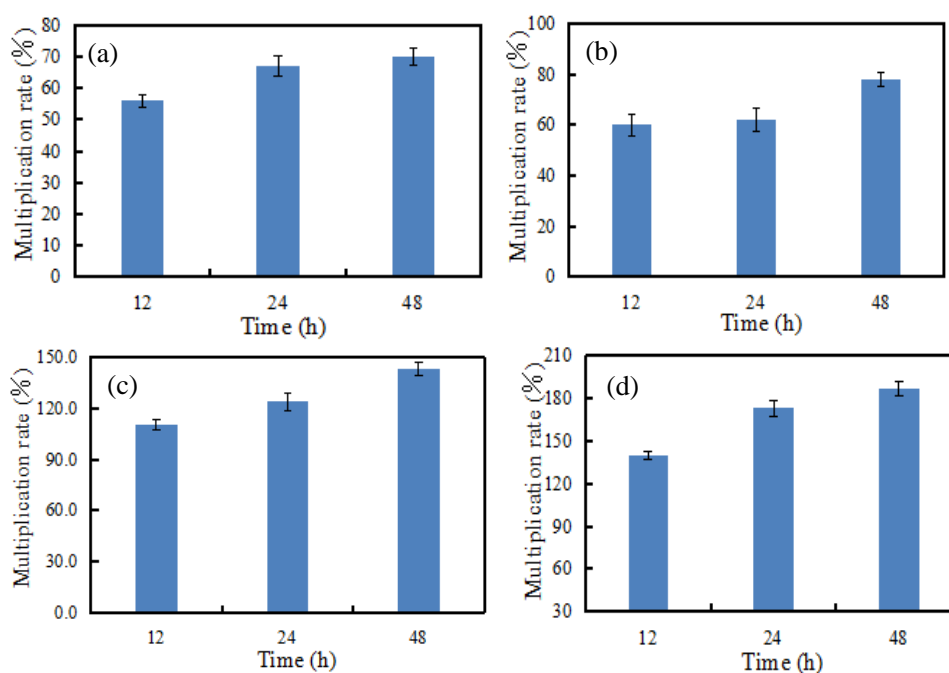


Figure 7. The proliferation index of different incubation time for different materials: (a) CaP-CS coating; (b) CaP-CS-GO coating; (c) CaP-CS-GO/ASA coating by the physical drug loading; (d) CaP-CS-GO/ASA coating by SC-CO₂ drug loading

Osteoblasts played an important role in the formation of bone and were responsible for the secretion and mineralization of bone matrix[37-39]. The higher the proliferation index of osteoblasts, the better the osteogenesis of the material[40-41]. In conclusion, the osteogenesis of magnesium alloy matrix CaP-CS-GO/ASA was better than that of magnesium alloy matrix CaP-CS-GO. In order to further investigate the effect of culture time on the osteogenesis of magnesium alloy matrix CaP-CS-GO/ASA, the culture time was extended to 3 days. It could be seen from Fig. 8 that the proliferation index of CaP-CS-GO/ASA coating by the physical drug group slowly increased when the culture time increased from 1~3 days, while the proliferation index of CaP-CS-GO/ASA coating by SC-CO₂ drug loading group significantly increased, and the proliferation index of the latter was significantly higher than that of the former. When soaking for 3 days, the proliferation index of CaP-CS-GO/ASA coating by the physical drug group was 152%, and that of CaP-

CS-GO/ASA coating by SC-CO₂ drug loading group was 192%. Thus, with the extension of soaking time, CaP-CS-GO/ASA coating still had good effect of proliferation and biocompatibility. Moreover, the higher the drug content in CaP-CS-GO/ASA coating group, the more conducive to the proliferation of osteoblasts, and the better the osteogenesis of materials were.

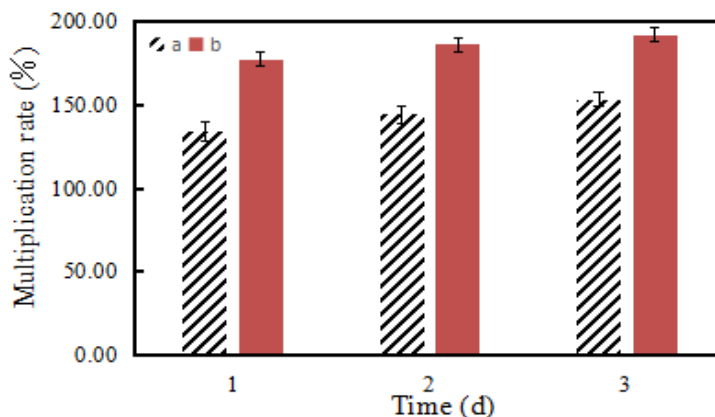
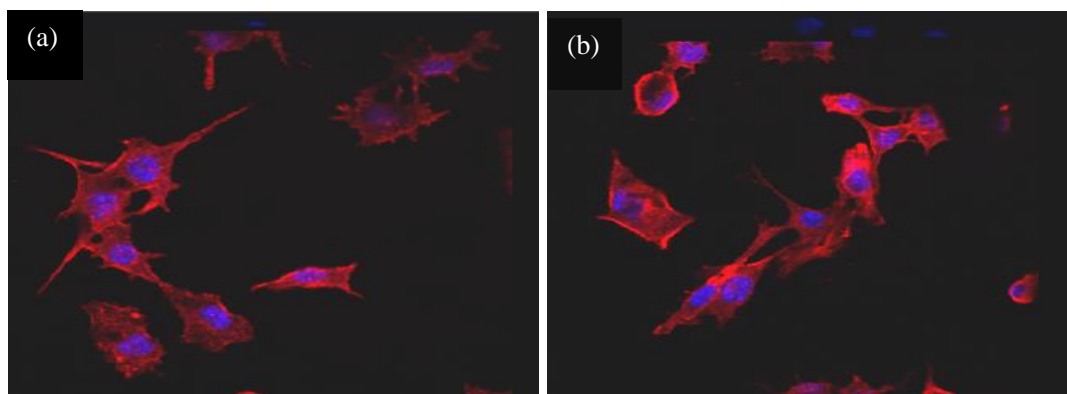


Figure 8. The proliferation index of different culture time for different materials: (a) CaP-CS-GO/ASA coating by the physical drug loading; (b) CaP-CS-GO/ASA coating by SC-CO₂ drug loading

3.5 Results of confocal laser

The testing results of confocal laser with CaP-CS coating, CaP-CS-GO coating, CaP-CS-GO/ASA coating by the physical drug loading and CaP-CS-GO/ASA coating by SC-CO₂ drug loading were shown in Fig.9. As Fig.9 illustrated, the cell shape in the four groups was irregular. Most of them were triangular, polygonal, with many protuberant, single nucleus, and the nucleus was oval. The cell matrix was wrapped around the nucleus, and the intercellular pseudopodia fused with each other, which indicated that the cells all grew on four kinds of membrane matrix. Compared with CaP-CS coating (Fig.9 (a)) and CaP-CS-GO coating (Fig.9 (b)), the number of osteoblasts on CaP-CS-GO/ASA coating (Fig.9 (c) (d)) was significantly increased, which was because aspirin in the coating could promote cell proliferation and differentiation. In addition, the amount of drug-loading capacity in the CaP-CS-GO/ASA coating by SC-CO₂ drug loading (Fig.9(d)) was higher than CaP-CS-GO/ASA coating by the physical drug loading (Fig.9(c)). Therefore, the number of osteoblast on CaP-CS-GO/ASA coating by SC-CO₂ drug loading was the highest .



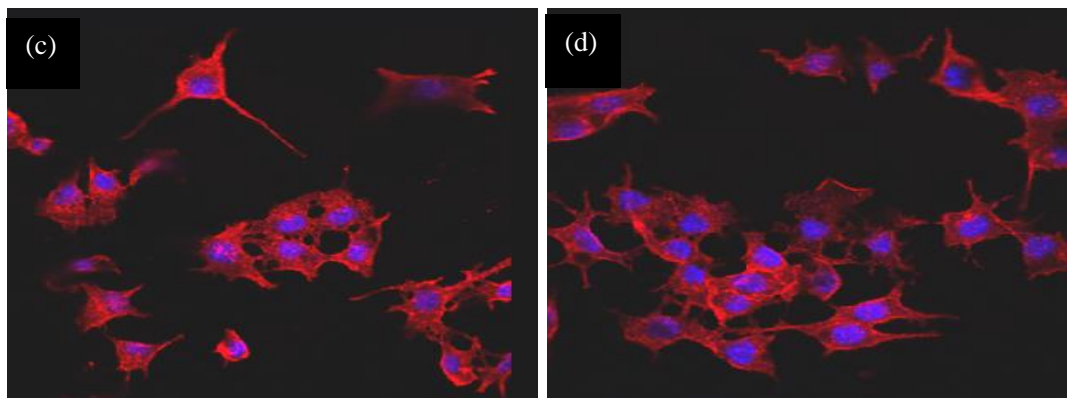


Figure 9. Laser confocal maps of different coatings: (a) CaP-CS coating; (b) CaP-CS-GO coating; (c) CaP-CS-GO/ASA coating by the physical drug loading; (d) CaP-CS-GO/ASA coating by SC-CO₂ drug loading

4. CONCLUSION

These characteristics of high diffusibility and the disappearance of gas-liquid interface of SC-CO₂ were used to load aspirin on GO, then the CaP-CS-GO/ASA coating by SC-CO₂ drug loading was prepared on magnesium alloy matrix by the method of electrophoretic deposition. The obtained bone material of magnesium alloy matrix CaP-CS-GO/ASA coating by SC-CO₂ drug loading has excellent biological activity and suitable degradation rate, it could promote the proliferation of mouse osteoblasts 3T3E1, which was osteogenic.

ACKNOWLEDGEMENTS

This work was supported by National Natural Science Foundation of China (No. 81601616), Excellent innovation team based on the basic scientific research vocational cost for the provincial undergraduate universities in Heilongjiang province (No. 2018-KYYWF-0914).

References

1. N. Fu, T. Dong, A. Meng, Z. Meng, B. Zhu And Y. Lin. *Curr Stem Cell Res Ther.*, 13 (2018) 583.
2. E. Zhang, L. Xu, G. Yu, F. Pan And K. Yang. *J Biomed Mater Res A.*, 90 (2009) 882.
3. W. Zhao, Z. Xu, Q. Cui And N. Sahai. *Langmuir.*, 32 (2016) 7009.
4. C. Li, B. Wang, X. Liu, Z. Pan, C. Liu, H. Ma, X. Liu, L. Liu And C. Jiang. *Artif Cells Nanomed Biotechnol.*, 47 (2019) 1823.
5. W. Kozuma, K. Kon, S. Kawakami, A. Bobothike, H. Iijima, M. Shiota And S. Kasugai. *Dent Mater J.*, 38 (2019) 771.
6. R. Thenmozhi, M.S. Moorthy, J. Sivaguru, P. Manivasagan, S. Bharathiraja And Y.O. Oh, J. Oh. *J Nanosci Nanotechnol.*, 19 (2019) 1951.
7. J. Du, Y. Zuo, L. Lin, D. Huang, L. Niu, Y. Wei, K. Wang, Q. Lin, Q. Zou And Y. Li. *J Mech Behav Biomed Mater.*, 88 (2018) 150.

8. A. Palaveniene, S. Tamburaci, C. Kimna, K. Glambaite, O. Baniukaitiene, F. Tihminlioğlu And J. Liesiene. *J Biomater Appl.*, 33 (2019) 876.
9. J. Hu, C. Wang, W.C. Ren, S. Zhang And F. Liu. *Mater Chem Phys.*, 119 (2010) 294.
10. J. Suh And H. Matthew. *Biomaterials*, 21 (2000) 2589.
11. K. Yin, P. Divakar And U.G.K. Wegst. *Biomacromolecules*, 20 (2019) 3733.
12. D. George, P.U. Maheswari, K.M.M. Sheriffa Begum And G. Arthanareeswaran. *J Agric Food Chem.*, 67 (2019) 10880.
13. M. Kalbacovaa, A Broza, J. Kong And M. Kalbac. *Carbon.*, 48 (2010) 4323.
14. J. Park, A. Fertala And R.E. Tomlinson. *Bone.*, 124 (2019) 22.
15. L. Zhang, W.W. Liu, C.G. Yue, T.H. Zhang, P. Li, Z.W. Xing And Y. Chen. *Carbon.*, 61 (2013) 105.
16. E. Kopp, S. Ghosh. *Science*, 265 (1994) 959.
17. S.M. Bode-Böger, J. Martens-Lobenhoffer, M. Täger, H. Schröder And F. Scalera. *Biochem Biophys Res Commun.*, 334 (2005) 1226.
18. Y Sun. *Curr Pharm Des.*, 20 (2014) 349.
19. T.N.M. Pham, T.B. Le, D.D. Le, T.H. Ha, N.S. Nguyen, T.D. Pham, P.C. Hauser, T.A.H. Nguyen And T.D. Mai. *J Pharm Biomed Anal.*, 178 (2019) 112906.
20. J. Zhang, Z.H. Wen, M. Zhao, G.Z. Li And C.S. Dai. *Mater Sci Eng C Mater Biol Appl.*, 58 (2016) 992.
21. J. Zhang, C.S. Dai, J. Wei, Z.H. Wen, S.J. Zhang And C. Chen. *Colloids Surf B Biointerfaces*, 111 (2013) 179.
22. M. Bahu, B.P. Knight, R. Weiss, S.J. Hahn, R. Goyal, E.G. Daoud, K.C. Man, F. Morady And S.A. Strickberger. *J Interv Card Electrophysiol.*, 2 (1998) 41.
23. S. Sagadevan, A.R. Marlinda, M.R. Johan, A. Umar, H. Fouad, O.Y. Alothman, U. Khaled, M.S. Akhtar And M.M. Shahid. *J Colloid Interface Sci.*, 558 (2019) 68.
24. A. Kowalczyk, U.X. Silva Neto, L.F. Fariniuk, V.P.D. Westphalen, C.A.H. Laurindo And E. Carneiro. *Int Endod J.*, 50 (2017) 578.
25. Y.K. Pan, C.Z. Chen, D.G. Wang And T.G. Zhao. *Colloids Surf B Biointerfaces*, 109 (2013) 1.
26. J. Zhang, F.F. Zhu, Y. Zhang, M. Hu, Y.X. Chi, X.Y. Zhang And X.L. Guo. *Int. J. Electrochem. Sci.*, 11 (2016) 9326.
27. B. Leclercq, L.Y. Alleman, E. Perdrix, V. Riffault, M. Happillon, A. Strecker, J.M. Lo-Guidice, G. Garçon And P. Coddeville. *Environ Res.*, 156 (2017) 148.
28. T.S. Frantz, N.J. Silveira, M.S. Quadro, R. Andrezza, A.A. Barcelos, T.R.S.J. Cadaval And L.A.A. Pinto. *Environ Sci Pollut Res Int.*, 24 (2017) 5908.
29. M.B. Kannan And R.K. Raman. *Biomaterials*, 29 (2008) 2306.
30. H. Qu And M. Wei. *J Biomed Mater Res B Appl Biomater.*, 84 (2008) 436.
31. Y. Liu, M. Li, Z. Yin, S. Zhou And Y. Qiu. *Cell Biol Int.*, 23 (2019) 11256.
32. H.F. Hozyen, E.S. Ibrahim, E.A. Khairy And S.I. El-Dek. *Vet World*, 12 (2019) 1225.
33. T. Sato, S. Kokabu, Y. Enoki, N. Hayashi, M. Matsumoto, M. Nakahira, M. Sugawara And T. Yoda. *In Vivo*, 31 (2017) 321.
34. Y. Han, F. Zhang, J. Zhang, D. Shao, Y. Wang, S. Li, S. Lv, G. Chi, M. Zhang, L. Chen And J. Liu. *Colloids Surf B Biointerfaces*, 179 (2019) 1.
35. L. Ren, S. Pan, H. Li, Y. Li, L. He, S. Zhang, J. Che And Y. Niu. *Sci Rep.*, 8 (2018) 15143.
36. M.C. Aisa, A. Datti, A. Orlacchio And G.C.D. Renzo. *Life Sci.*, 208 (2018) 10.
37. V.J. Woeckel, R.D. Alves, S.M. Swagemakers, M. Eijken, H. Chiba, B.C. van der Eerden And J.P. van Leeuwen. *J Cell Physiol.*, 225 (2010) 593.
38. A. Strzelecka-Kiliszek, L. Bozycki, S. Mebarek, R. Buchet And S. Pikula. *J Inorg Biochem.*, 171 (2017) 100.
39. A. Strzelecka-Kiliszek, S. Mebarek, M. Roszkowska, R. Buchet, D. Magne And S. Pikula. *Pikula S.Biochim Biophys Acta Gen Subj.*, 1861 (2017) 1009.
40. A. Sujana, J.R. Venugopal, B. Velmurugan, A. Góra, M. Salla And S. Ramakrishna. *J Tissue Eng Regen Med.*, 11 (2017) 1853.

41. J. Venugopal, M.P. Prabhakaran, Y. Zhang, S. Low, A.T. Choon And S. Ramakrishna. *Philos Trans A Math Phys Eng Sci.*, 368 (2010) 2065.

© 2020 The Authors. Published by ESG (www.electrochemsci.org). This article is an open access article distributed under the terms and conditions of the Creative Commons Attribution license (<http://creativecommons.org/licenses/by/4.0/>).